

# Geometry-Contrastive Generative Adversarial Network for Facial Expression Synthesis

Fengchun Qiao<sup>1</sup>, Naiming Yao<sup>1</sup>, Zirui Jiao<sup>1</sup>, Zhihao Li<sup>1</sup>, Hui Chen<sup>1</sup>, Hongan Wang<sup>1</sup>,

<sup>1</sup> Institute of Software, Chinese Academy of Sciences

## Abstract

In this paper, we propose a geometry-contrastive generative adversarial network *GC-GAN* for generating facial expression images conditioned on geometry information. Specifically, given an input face and a target expression designated by a set of facial landmarks, an identity-preserving face can be generated guided by the target expression. In order to embed facial geometry onto a semantic manifold, we incorporate contrastive learning into conditional *GANs*. Experiment results demonstrate that the manifold is sensitive to the changes of facial geometry both globally and locally. Benefited from the semantic manifold, dynamic smooth transitions between different facial expressions are exhibited via geometry interpolation. Furthermore, our method can also be applied in facial expression transfer even there exist big differences in face shape between target faces and driving faces.

## 1 Introduction

Facial expression synthesis aims to generate identity-preserving faces conditioned on specific emotion states. A wide range of applications in affective interaction, such as facial animation, facial editing, and facial expression recognition, could be facilitated by the advances of facial expression synthesis. In the past few decades, traditional computer graphics techniques are dominant in this field. Numerous graphic-based methods manipulate existing patches or resort to 3D-based techniques at pixel level rather than at semantic level. However, facial expression synthesis remains enduring challenges at semantic level due to the high nonlinearity of facial expression changes and variances of individuals. How to apply semantic information in guiding the synthesis of facial expressions is still an open problem.

Facial expression synthesis is closely connected with face animation. Some representative works on face animation, e.g. [Dale *et al.*, 2011] and [Thies *et al.*, 2016], usually assume the availability of a video of the target face with variants in facial expressions and head poses, which limits their applications. Recently, [Averbuch-Elor *et al.*, 2017] proposed a warp-based method to animate a single facial image and

to transfer invisible regions seamlessly. This method generates both photo-realistic and high-resolution facial expression videos, just like bringing a still portrait to life. It assumes that the target face and the start frame of a driving video are both neutral faces in frontal pose, however, the neutral faces are not always available in the practical environment. In contrast to previous studies, neutral faces are not required in our model. Additionally, we can exhibit the smooth transition between different facial expressions through geometry interpolation.

With the recent development of generative adversarial nets (*GANs*), image synthesis has migrated from pixel-level manipulations to semantic manipulations [Zhou and Shi, 2017]. *GANs* have also been widely applied in face-related tasks, such as face pose manipulation [Yin *et al.*, 2017], face aging [Zhang *et al.*, 2017b], and facial expression synthesis [Zhou and Shi, 2017; Choi *et al.*, 2017]. However, existing works relating to *GANs*-based facial expression synthesis mainly focus on generating facial expressions of annotated categories in facial expression datasets.

From the perspective of psychology, facial expressions are explained as combinations of muscle movements underneath the skin of the face, and these muscle movements are encoded as a set of action units (*AU*) in the Facial Action Coding System (*FACS*) [Ekman and Friesen, 1977]. *AU* can be represented in the form of appearance features or geometry features. For this reason, facial landmarks are regarded as guiding information in facial expression synthesis in our method, and we can generate more facial expressions than basic types.

In this paper, we propose *GC-GAN*, a geometry-contrastive generative adversarial network, for synthesizing facial expression images conditioned on geometry information at semantic level. *GC-GAN* consists of a facial geometry embedding network, an image generator network, and an image discriminator network. In particular, the geometry embedding network is used to map facial landmarks onto a semantic manifold in latent space by contrastive learning. Through visualization and experimental results, we demonstrate that the embedded manifold is semantic-aware and suitable for more facial expression characteristics. The main contributions of the paper are summarized as follows:

- We inject geometry information into conditional *GANs* in a novel way, which can guide the synthesis of facial expressions.

- We combine contrastive learning with adversarial learning to embed facial geometry onto a semantic manifold, during which the potentials of existing categorical facial expression datasets are fully explored.
- Experimental results demonstrate that our proposed method can be applied in natural facial expression transfer even there exist big differences in face shape between target faces and driving faces.

## 2 Related work

**Conditional Generative Adversarial Networks.** Following the emergence of generative adversarial nets (GANs) [Goodfellow *et al.*, 2014], GANs-based conditional image generation has been actively studied. [Mirza and Osindero, 2014] proposed conditional GANs to generate images controlled by labels or attributes. [Larsen *et al.*, 2016] combined variational autoencoder (VAE) and GANs to learn an embedding representation which can be used to modify high-level abstract visual features by simple arithmetic. GANs have also been applied in facial expression synthesis [Zhou and Shi, 2017; Choi *et al.*, 2017; Gu *et al.*, 2017]. [Zhou and Shi, 2017] proposed a conditional difference adversarial autoencoder (CDAAE) to generate faces conditioned on emotion classes or AU labels. [Choi *et al.*, 2017] proposed *StarGAN* to perform image-to-image translations for multiple domains using only a single model, which can also be applied in facial expression synthesis. Previous studies mainly focus on generating facial images conditioned on discrete emotion classes. However, human emotion is expressed in a continuous way, thus discrete labels are not sufficient to describe detailed characteristics of facial expressions.

**Geometry Guided Generative Adversarial Networks.** Recently, some researchers have attempted to incorporate continuous information such as geometry into conditional GANs [Ma *et al.*, 2017; Song *et al.*, 2017; Kossaihi *et al.*, 2017]. [Ma *et al.*, 2017] proposed a pose guided person generation network  $PG^2$ , which allows to generate images of individuals in arbitrary poses. The target pose is defined by a set of 18 joint locations and encoded as heatmaps, which are concatenated with the input image in  $PG^2$ . In addition, they adopted a two-stage generation method to enhance the quality of generated images. [Song *et al.*, 2017] proposed a geometry guided generative adversarial network (G2GAN), which applies facial geometry information to guiding the synthesis of facial expressions. The facial landmarks are treated as an additional image channel to be concatenated with the input face directly. They use dual generators to perform the synthesis and the removal of facial expressions simultaneously. The neural facial images are generated through the removal network and used for the subsequent facial expression transfer. This procedure brings additional artifacts and degrades the performance especially when the driving faces are collected from other subjects in different datasets. In our method, the features of facial identity and facial expression are learned in a disentangled way, and facial landmarks are mapped onto a semantic manifold through a geometry embedding network adapting for unseen facial expression characteristics.

## 3 The Proposed Approach

In this section, we present the pipeline of the proposed geometry-contrastive generative adversarial network (GC-GAN).

We use  $I_i^e$  and  $g_i^e$  to represent a facial image and a facial geometry respectively, and the superscripts  $e$  indicates an emotion state while the subscripts  $i$  denotes an identity. Given a source facial image  $I_i^u$  and a target facial expression  $g_i^v$  represented by a set of facial landmarks, GC-GAN aims to generate a new identity-preserving facial image  $\hat{I}_i^v$  conditioned on the target facial expression.

The overall framework of GC-GAN is shown in Fig. 1. GC-GAN consists of three components: a facial geometry embedding network  $E$ , an image generator network  $G$ , and an image discriminator network  $D$ . Input facial image  $I_i^u$  and target landmarks  $g_i^v$  are encoded by  $G_{enc}$  and  $E_{enc}$  into  $z_i$  and  $z_g$  respectively. Then  $z_i$  and  $z_g$  are concatenated into a single vector  $z$  for  $G_{dec}$ .  $g_{(\cdot)}^{ref}$  is reference facial landmarks used for contrastive learning against  $g_i^v$ . Note that expression features  $z_g$  and identity features  $z_i$  are learned in a disentangled manner, thus we could modify expression and keep identity preserved. GC-GAN is trained in a multi-task way where contrastive learning, adversarial learning, and reconstruction learning are utilized.

### 3.1 Contrastive Learning

Facial landmarks provide the basic geometry information and expression information of faces. Besides, facial landmarks can be naturally adopted as control points in face-editing tasks. Moreover, facial landmarks of the same expression share similar characteristics. To some degree, the intra-class similarities of the facial landmarks can be used to construct a semantic manifold. To achieve this goal, reference facial landmarks are introduced to conduct contrastive learning against target facial landmarks [Zhang *et al.*, 2017a]. In detail, the  $xy$ -coordinates of facial landmarks are arranged into a one-dimensional vector as input for the geometry embedding network. Landmark pairs  $(g_{(\cdot)}^v, g_{(\cdot)}^{ref})$  are prepared for training, in which  $g_{(\cdot)}^v$  is the target expression,  $g_{(\cdot)}^{ref}$  is the reference expression and  $(\cdot)$  represents a certain subject. After a transform function  $E_{enc}(\cdot)$ , the facial landmarks are mapped into the embedding space. Our goal is to measure the similarity between  $E_{enc}(g_{(\cdot)}^v)$  and  $E_{enc}(g_{(\cdot)}^{ref})$  according to their expression labels. The contrastive loss  $L_{contr}$  is formulated as below:

$$\min_{E_{enc}} L_{contr} = \frac{\alpha}{2} \max \left( 0, m - \left\| E_{enc}(g_{(\cdot)}^v) - E_{enc}(g_{(\cdot)}^{ref}) \right\|_2 \right)^2 + \frac{1-\alpha}{2} \left\| E_{enc}(g_{(\cdot)}^v) - E_{enc}(g_{(\cdot)}^{ref}) \right\|_2^2, \quad (1)$$

where  $\alpha = 0$ , if the expression labels are the same,  $\alpha = 1$  otherwise.  $m$  is a margin which is always greater than 0.  $L_{contr}$  enables our embedding network to focus on facial expression itself regardless of different subjects and plays an essential part for the construction of the semantic manifold of facial landmarks. We will explain it in detail in Sec. 4.3.

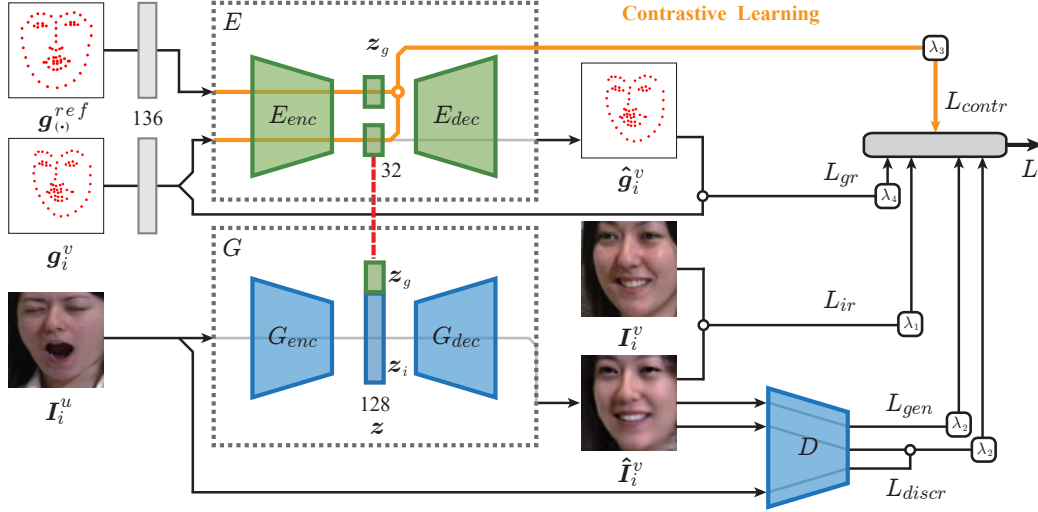


Figure 1: Overview of the GC-GAN framework. The GC-GAN consists of three components: a facial geometry embedding network  $E$ , an image generator network  $G$ , and an image discriminator network  $D$ . Input facial image  $I_i^u$  and target landmarks  $g_i^v$  are encoded by  $G_{enc}$  and  $E_{enc}$  into  $z_i$  and  $z_g$  respectively. Then  $z_i$  and  $z_g$  are concatenated into a single vector  $z$  for  $G_{dec}$ .  $g_{(\cdot)}^{ref}$  is reference facial landmarks used for contrastive learning against  $g_i^v$ .

### 3.2 Adversarial Learning

The min-max game between generator  $G$  and discriminator  $D$  is introduced to make the generated image visually realistic. The objective of original GANs is formulated as follows:

$$\min_G \max_D L_{GAN} = \mathbb{E}[\log D(x)] + \mathbb{E}[\log(1 - D(G(z)))], \quad (2)$$

where  $x$  and  $z$  are the distributions of real data and Gaussian noise. In our model, the adversarial losses for the  $G$  and  $D$  are formulated as follows:

$$\min_D L_{discr} = -\mathbb{E}_{I \sim p_I} D(I_i^u) + \mathbb{E}_{I \sim p_I, g \sim p_g} D(\hat{I}_i^v), \quad (3)$$

$$\min_{G, E_{enc}} L_{gen} = -\mathbb{E}_{I \sim p_I, g \sim p_g} D(\hat{I}_i^v), \quad (4)$$

$$\min_{G, E_{enc}, D} L_{adv} = L_{discr} + L_{gen}, \quad (5)$$

where  $p_I$  and  $p_g$  indicate the distribution of real facial images and real facial landmarks.  $\hat{I}_i^v$  represents  $G_{dec}(G_{enc}(I_i^u), E_{enc}(g_i^v))$ . The adversarial losses are optimized via WGAN-GP [Gulrajani et al., 2017].

### 3.3 Reconstruction Learning

Apart from the most important losses mentioned in Sec. 3.1 and Sec. 3.2,  $\ell_1$  loss and  $\ell_2$  loss are introduced for the reconstruction of faces and landmarks, respectively. For the generated facial image  $\hat{I}_i^v$ , we employ  $\ell_1$  distance to compute a pixel-to-pixel difference between generated image and target real image, which is formulated as below:

$$\min_{G, E_{enc}} L_{ir} = \|I_i^v - \hat{I}_i^v\|_1. \quad (6)$$

Compared with  $\ell_2$  loss,  $\ell_1$  loss preserves high frequency signals better and suppresses blur. The mixture of adversarial loss and  $L_{ir}$  accelerate the convergence and enhance image

visual quality. For facial landmarks, we employ  $\ell_2$  distance to compute the difference between reconstructed landmarks and input landmarks, which is formulated as below:

$$\min_E L_{gr} = \|g_i^v - \hat{g}_i^v\|_2^2. \quad (7)$$

Reconstruction learning enables latent vector  $z$  to preserve enough information for the reconstruction of inputs.

### 3.4 Overall Objective

The joint objective is computed by combining Eqs. (1), (5), (6), and (7) as follow:

$$\min_{G, D, E} L = \lambda_1 L_{ir} + \lambda_2 L_{adv} + \lambda_3 L_{contr} + \lambda_4 L_{gr}, \quad (8)$$

where  $\lambda_1$ ,  $\lambda_2$ ,  $\lambda_3$ , and  $\lambda_4$  are the weights of the losses.

### 3.5 Network Architectures and Settings

The generator network  $G$  has a similar architecture to *U-Net* [Li and Wand, 2016]. Different from the original *U-Net*, we only add one skip connection between the output of the first convolution layer and the output of the penultimate deconvolution layer, which enables  $G$  to reuse low-level facial features related with identity information. For discriminator network  $D$ , the output is a  $2 \times 2$  feature map which is similar to [Shrivastava et al., 2017]. Table 1 shows the detailed network architectures of our GC-GAN. The margin  $m$  in  $L_{contr}$  is set to 5. The coefficients  $\lambda_1$ ,  $\lambda_2$ ,  $\lambda_3$ , and  $\lambda_4$  in the loss  $L$  are empirically set to 1,  $10^{-3}$ ,  $10^{-4}$  and  $10^{-4}$ , respectively. All the networks  $E$ ,  $G$ , and  $D$  are trained jointly in a multi-task way by using the *Adam* optimizer [Kingma and Ba, 2014] with  $\beta_1 = 0.5$  and  $\beta_2 = 0.999$ . The batch size is 64 and the initial learning rate is set to  $3 \times 10^{-4}$ . We implement GC-GAN using *Tensorflow* [Abadi et al., 2016].

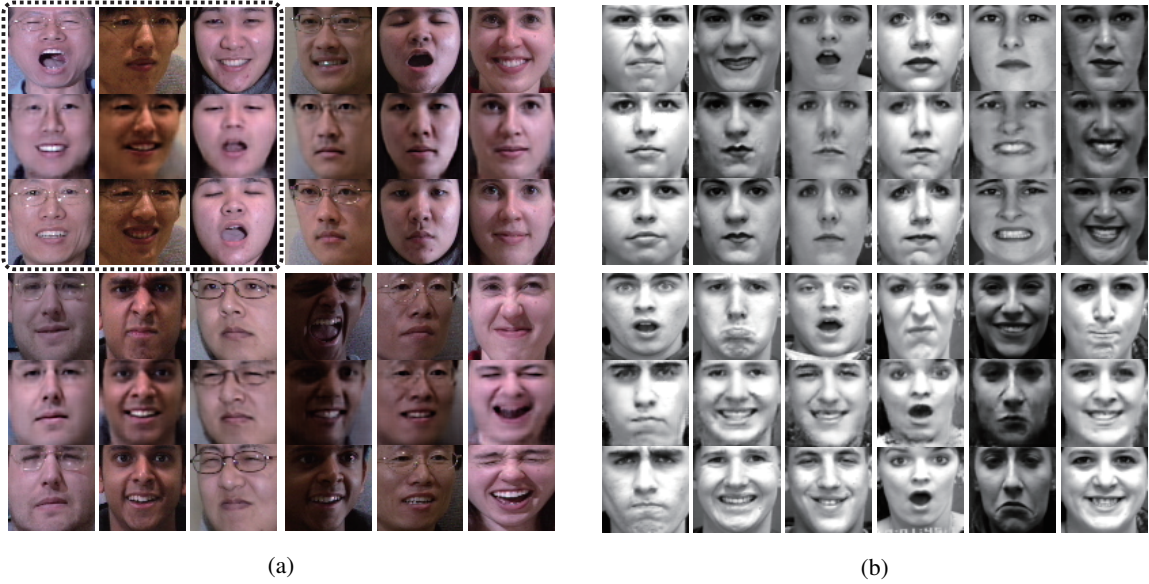


Figure 2: Results of facial expression synthesis on (a) *Multi-PIE* and (b) *CK+*. Three images from top to bottom in each column represent the input image, generated image, and ground truth, respectively.

Table 1: The detailed architecture of *GC-GAN*. In  $(De)Conv(d,k,s)$ ,  $d$ ,  $k$ , and  $s$  stand for the number of filters, the kernel size, and the stride, respectively. *FC* represents a fully-connected layer. *BN* is batch normalization and *LN* is layer normalization. *LReLU* refers to *leaky ReLU*.

Embedding $E$	Generator $G$
FC(128), BN, ReLU	Conv(64,5,2), BN, ReLU
FC(64), BN, ReLU	Conv(128,5,2), BN, ReLU
FC(32), BN, ReLU	Conv(256,5,2), BN, ReLU
FC(64), BN, ReLU	FC(1024), BN, ReLU
FC(128), BN, ReLU	FC(128), BN, ReLU
FC(136), Tanh	FC(4096), BN, ReLU
Discriminator $D$	DeConv(256,5,2), BN, ReLU
Conv(64,5,2), LN, LReLU	DeConv(128,5,2), BN, ReLU
Conv(128,5,2), LN, LReLU	DeConv(64,5,2), BN, ReLU
Conv(256,5,2), LN, LReLU	DeConv(64,5,2), BN, ReLU
Conv(512,5,2), LN, LReLU	Conv(3,5,1), BN, Tanh
Conv(1,5,2)	

## 4 Experiments

### 4.1 Datasets and Protocols

To evaluate the proposed *GC-GAN*, we conduct extensive experiments on two popular facial expression datasets: *Multi-PIE* [Gross *et al.*, 2010] and *CK+* [Lucey *et al.*, 2010]. And *CelebA* [Liu *et al.*, 2015] is used in facial expression transfer.

*Multi-PIE* is a challenging facial expression dataset, which consists of 754,200 images from 337 subjects with large variations in head pose, illumination, and facial expression. We select a subset of images with 3 head poses ( $0^\circ, \pm 15^\circ$ ), 20 illumination conditions, and all 6 expressions (neural, smile, surprise, squint, disgust, and scream). Input images and target images are under the same conditions of pose and illumination. The training set and test set are split based on subjects

with proportion of 90% and 10%, respectively.

*CK+* is a representative database for facial expression recognition, composing of 327 image sequences with seven prototypical emotion labels, namely, anger, contempt, disgust, fear, happiness, sadness, and surprise. Each sequence starts with a neutral emotion and ends with the peak of a certain emotion. There are 118 subjects in this dataset. Following the widely-adopted protocol introduced in [Zhang *et al.*, 2017a], these subjects are grouped into ten subsets by ID and nine subsets are used for training while the remaining subset is used for test.

*CelebA* is a large-scale facial dataset, containing 202,599 face images of celebrities, each of which is annotated with 40 binary attributes.

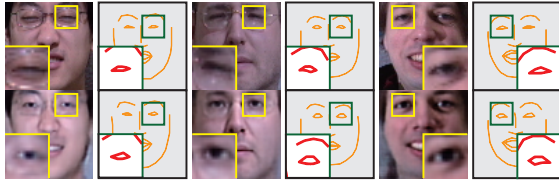
To prepare the training pairs  $(I_i^u, I_i^v, g_i^v)$ , we create all pairs of facial expressions per identity and generate the reference landmarks  $g_{(\cdot)}^{ref}$  by sampling at random. Note that the reference landmarks  $g_{(\cdot)}^{ref}$  are not required in test. In our experiments, the facial landmarks are obtained through *dlib*<sup>1</sup> and the number is 68 in total including landmark points of two eyebrows, two eyes, the nose, the lips, and the jaw. The facial images are aligned based on inner eyes and bottom lip. Then, face regions are cropped and resized into  $64 \times 64$ . Image values and  $xy$ -coordinates of facial landmarks are both normalized into  $[-1, 1]$ .

### 4.2 Facial Expression Synthesis

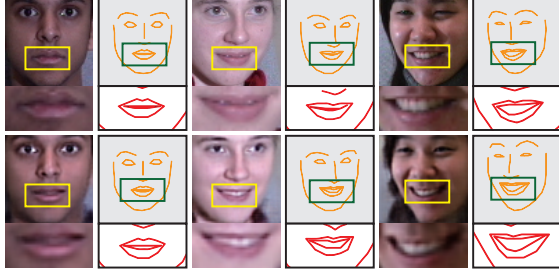
In order to evaluate whether the synthetic faces are generated conditioned on target expression, we qualitatively and quantitatively compare the generated faces with the ground truth. The qualitative results are shown in Fig. 2, in which the generated faces are identity-preserving and are similar to

<sup>1</sup><http://dlib.net/>





(a)



(b)

Figure 3: Generated faces by local modification of facial landmarks. Two images from top to bottom in each column represent the input image and generated image, and the modified regions are emphasized. Modifications of eyes and mouth are shown in (a) and (b) respectively. The corresponding facial landmarks are shown next to each image.

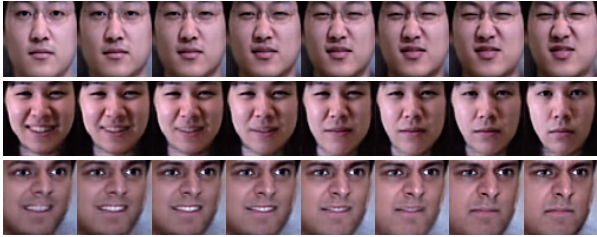
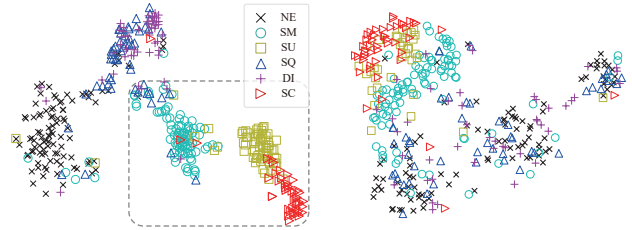


Figure 4: Smooth transitions of facial expressions on *Multi-PIE* achieved by geometry interpolation from one facial expression to the other. The three rows show the facial expression transitions from *neutral* to *disgust*, from *smile* to *neutral*, and from *smile* to *disgust*, respectively.

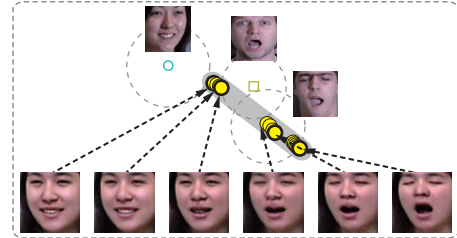
the target expressions, indicating the effectiveness of guiding facial landmarks. Besides, our method also hallucinates invisible parts of input faces such as pupils, teeth and tongue, which is shown in the top left corner of Fig. 2(a). In order to quantitatively measure the result, two evaluation metrics including *SSIM* (structural similarity index measure) and *PSNR* (peak-signal-to-noise ratio), are used. The detailed comparison results are shown in Table 2. We conduct ablation study to evaluate contributions of three losses  $L_{ir}$ ,  $L_{gr}$ , and  $L_{contr}$ , respectively. According to Table 2, *GC-GAN* performs better supervised by the three losses. *G2GAN* [Song *et al.*, 2017] is the most similar work to ours as far as we know. In their work, the quantitative results of *Multi-PIE* are not given, so we compare our results with *G2GAN* on *CK+*. As shown in Table 2, our method outperforms *G2GAN* in both measures.

The experiments mentioned above demonstrate that our proposed *GC-GAN* effectively incorporates geometry information in conditioned facial expression synthesis. In order to evaluate whether *GC-GAN* is capable of reacting to the local



(a)

(b)



(c)

Figure 5: Visualization of the semantic manifold. (a) shows the embedding manifold of facial landmarks in the test set of *Multi-PIE*. NE, SM, SU, SQ, DI, and SC, which are abbreviated in the legend, stand for *neural*, *smile*, *surprise*, *squint*, *disgust*, and *scream*, respectively. (b) shows the embedding manifold obtained without contrastive learning. (c). The embedding points in yellow correspond to the expression transition from *smile* to *scream* of the same person. Apart from the yellow points, the centers of neighbor expressions are also presented.

Table 2: Comparison with other settings and method on *Multi-PIE* and *CK+* in terms of *SSIM* and *PSNR*.

	<i>Multi-PIE</i>		<i>CK+</i>	
	<i>SSIM</i>	<i>PSNR</i>	<i>SSIM</i>	<i>PSNR</i>
<i>GC-GAN</i> (ours)	0.687	26.731	<b>0.769</b>	<b>27.665</b>
w/o $L_{ir}$	0.663	25.917	0.756	26.781
w/o $L_{gr}$	0.682	26.701	0.768	27.463
w/o $L_{contr}$	0.675	26.433	0.763	27.325
<i>G2GAN</i>	-	-	0.767	24.420

changes of facial landmarks, we manually modify the positions of local facial landmarks and feed them into embedding network  $E$ . The results are shown in Fig. 3. In detail, we conduct two types of local modification of facial landmarks: eyes enlarging and uplift of corners of mouth. For the former one, we raise landmark points of upper eyelids by 2 pixels and lower the lower eyelids by 2 pixels, and the corresponding results are shown in Fig. 3(a). For the latter one, we raise landmark points of mouth corners by 2 pixels, and the corresponding results are shown in Fig. 3(b). The results of our experiments indicate that the embedded feature  $z_g$  is capable of capturing changes of local facial landmarks.

### 4.3 Effects of Geometry-Contrastive Learning

In order to evaluate whether there exists semantic correspondence between embedding space and geometry space of facial landmarks, geometry traversal is introduced for qualitative analysis and the embedded manifold is visualized for further exploration. For geometry traversal, we would like



Figure 6: Results of facial expression transfer on *Multi-PIE* for *CelebA*. (a) Input images. (b) Guiding facial geometry. (C) Driving faces. The guiding facial geometry are taken from the corresponding driving faces. (d) Generated faces by our method. (e) Generated faces by *SPG*.

to seek a sequence of  $N$  images with a smooth transition between two different facial expressions of the same person (e.g.  $I_i^u$  and  $I_i^v$ ). In our case, we conduct a linear interpolation  $[\frac{t}{N} \cdot g_i^u + (1 - \frac{t}{N}) \cdot g_i^v]_{t=0}^N$  on facial landmarks. Fig. 4 shows smooth transitions between different facial expressions. As shown in Fig. 4, each generated image sequence is just like a video recording the dynamic expression changes of a person.

Furthermore, we visualize the embedding manifold of facial landmarks by *t-SNE* [Maaten and Hinton, 2008]. As shown in Fig. 5(a), the embedding features are clustered according to their labels. We find that the data points of *disgust* and *squint* are mixed up with each other due to the intrinsic geometry similarity between the two facial expressions. In addition, we present an embedding line consisting of a sequence of points corresponding to the expression transition from *smile* to *scream* of the same person as shown in Fig. 5(c). We observe that from *smile* to *scream* the eyes are closing and the mouth is opening. So there could exist some points with open eyes and open mouth simultaneously which is exactly the characteristic of *surprise*, and could account for the reason why the embedding line comes across the region of *surprise*. In order to evaluate the effectiveness of contrastive learning, we retrain our model without contrastive loss  $L_{contr}$ . The corresponding manifold of facial landmarks is shown in Fig. 5(b), in which the embedding features cannot be clustered properly without the guidance of contrastive learning, indicating that adversarial learning alone is not sufficient to embed facial geometry onto a semantic manifold. The qualitative results and the visualization of the manifold indicate that the embedding space and geometry space of facial landmarks are semantically consistent.

#### 4.4 Facial Expression Transfer

To further evaluate the generality of our proposed geometry embedding network, we conduct a more challenging task: facial expression transfer. Facial expression transfer between different persons are difficult due to the individual variances,

especially in the absence of neutral faces for reference.

In our case, the target expressions are taken from other people of different datasets. Here, we randomly select 1000 facial images from *CelebA*. The facial landmarks of these images serve as guiding landmarks. Fig. 6(d) shows some representative samples from our experiment, in which the generated faces are identity-preserving and exhibit similar expressions with driving faces even there exist big differences in face shape between input faces and driving faces.

For comparison, we adopt a more general configuration similar to *PG<sup>2</sup>* [Ma *et al.*, 2017] and *G2GAN* [Song *et al.*, 2017], which is denoted as *SPG*. In detail, we treat the guiding landmarks as an additional feature map and directly concatenate it with the input face, and retrain our model in this configuration. The corresponding results are shown in Fig. 6(e). Compared with our method, this configuration is not able to capture the target expression of driving faces and brings extra artifact, indicating that this configuration cannot handle the misalignment between input faces and driving facial landmarks properly. The results demonstrate the superiority of our geometry embedding network in facial expression transfer.

## 5 Conclusion

In this paper, we have proposed geometry-contrastive generative adversarial network *GC-GAN* for generating facial expression images conditioned on geometry information. Through contrastive learning, we have constructed a semantic manifold to embed face geometry into a latent space and explored the potentials of limited emotion labels provided by facial expression datasets. Experimental results have demonstrated that the manifold is sensitive to the changes of facial geometry both globally and locally, and also suitable for unseen facial expression characteristics. Furthermore, our method can also be applied in facial expression transfer even there exist big differences in face shape between target faces and driving faces.

## References

- [Abadi *et al.*, 2016] Martín Abadi, Paul Barham, Jianmin Chen, Zhifeng Chen, Andy Davis, Jeffrey Dean, Matthieu Devin, Sanjay Ghemawat, Geoffrey Irving, Michael Isard, et al. TensorFlow: A system for large-scale machine learning. In *OSDI*, volume 16, pages 265–283, 2016.
- [Averbuch-Elor *et al.*, 2017] Hadar Averbuch-Elor, Daniel Cohen-Or, Johannes Kopf, and Michael F Cohen. Bringing portraits to life. *ACM Transactions on Graphics (TOG)*, 36(6):196, 2017.
- [Choi *et al.*, 2017] Yunjey Choi, Minje Choi, Munyoung Kim, Jung-Woo Ha, Sunghun Kim, and Jaegul Choo. Stargan: Unified generative adversarial networks for multi-domain image-to-image translation. *arXiv preprint arXiv:1711.09020*, 2017.
- [Dale *et al.*, 2011] Kevin Dale, Kalyan Sunkavalli, Micah K Johnson, Daniel Vlasic, Wojciech Matusik, and Hanspeter Pfister. Video face replacement. *ACM Transactions on Graphics (TOG)*, 30(6):130, 2011.
- [Ekman and Friesen, 1977] Paul Ekman and Wallace V Friesen. Facial action coding system. 1977.
- [Goodfellow *et al.*, 2014] Ian Goodfellow, Jean Pouget-Abadie, Mehdi Mirza, Bing Xu, David Warde-Farley, Sherjil Ozair, Aaron Courville, and Yoshua Bengio. Generative adversarial nets. In *Advances in Neural Information Processing Systems*, pages 2672–2680, 2014.
- [Gross *et al.*, 2010] Ralph Gross, Iain Matthews, Jeffrey Cohn, Takeo Kanade, and Simon Baker. Multi-PIE. *Image and Vision Computing*, 28(5):807–813, 2010.
- [Gu *et al.*, 2017] Geonmo Gu, Seong Tae Kim, Kihyun Kim, Wissam J Baddar, and Yong Man Ro. Differential generative adversarial networks: Synthesizing non-linear facial variations with limited number of training data. *arXiv preprint arXiv:1711.10267*, 2017.
- [Gulrajani *et al.*, 2017] Ishaan Gulrajani, Faruk Ahmed, Martin Arjovsky, Vincent Dumoulin, and Aaron Courville. Improved training of wasserstein gans. *arXiv preprint arXiv:1704.00028*, 2017.
- [Kingma and Ba, 2014] Diederik Kingma and Jimmy Ba. Adam: A method for stochastic optimization. *arXiv preprint arXiv:1412.6980*, 2014.
- [Kossaifi *et al.*, 2017] Jean Kossaifi, Linh Tran, Yannis Panagakis, and Maja Pantic. GAGAN: Geometry-aware generative adversarial networks. *arXiv preprint arXiv:1712.00684*, 2017.
- [Larsen *et al.*, 2016] Anders Boesen Lindbo Larsen, Søren Kaae Sønderby, Hugo Larochelle, and Ole Winther. Autoencoding beyond pixels using a learned similarity metric. In *International Conference on Machine Learning*, pages 1558–1566, 2016.
- [Li and Wand, 2016] Chuan Li and Michael Wand. Combining markov random fields and convolutional neural networks for image synthesis. In *Proceedings of the IEEE Conference on Computer Vision and Pattern Recognition*, pages 2479–2486, 2016.
- [Liu *et al.*, 2015] Ziwei Liu, Ping Luo, Xiaogang Wang, and Xiaoou Tang. Deep learning face attributes in the wild. In *Proceedings of the IEEE International Conference on Computer Vision*, pages 3730–3738, 2015.
- [Lucey *et al.*, 2010] Patrick Lucey, Jeffrey F Cohn, Takeo Kanade, Jason Saragih, Zara Ambadar, and Iain Matthews. The extended Cohn-Kanade dataset (CK+): A complete dataset for action unit and emotion-specified expression. In *2010 IEEE Computer Society Conference on Computer Vision and Pattern Recognition Workshops*, pages 94–101. IEEE, 2010.
- [Ma *et al.*, 2017] Liqian Ma, Xu Jia, Qianru Sun, Bernt Schiele, Tinne Tuytelaars, and Luc Van Gool. Pose guided person image generation. In *Advances in Neural Information Processing Systems*, pages 405–415, 2017.
- [Maaten and Hinton, 2008] Laurens van der Maaten and Geoffrey Hinton. Visualizing data using t-sne. *Journal of Machine Learning Research*, 9(Nov):2579–2605, 2008.
- [Mirza and Osindero, 2014] Mehdi Mirza and Simon Osindero. Conditional generative adversarial nets. *arXiv preprint arXiv:1411.1784*, 2014.
- [Shrivastava *et al.*, 2017] Ashish Shrivastava, Tomas Pfister, Oncel Tuzel, Josh Susskind, Wenda Wang, and Russ Webb. Learning from simulated and unsupervised images through adversarial training. In *The IEEE Conference on Computer Vision and Pattern Recognition (CVPR)*, volume 3, page 6, 2017.
- [Song *et al.*, 2017] Lingxiao Song, Zhihe Lu, Ran He, Zhenan Sun, and Tieniu Tan. Geometry guided adversarial facial expression synthesis. *arXiv preprint arXiv:1712.03474*, 2017.
- [Thies *et al.*, 2016] Justus Thies, Michael Zollhofer, Marc Stamminger, Christian Theobalt, and Matthias Nießner. Face2face: Real-time face capture and reenactment of rgb videos. In *Proceedings of the IEEE Conference on Computer Vision and Pattern Recognition*, pages 2387–2395, 2016.
- [Yin *et al.*, 2017] Xi Yin, Xiang Yu, Kihyuk Sohn, Xiaoming Liu, and Manmohan Chandraker. Towards large-pose face frontalization in the wild. *arXiv preprint arXiv:1704.06244*, 2017.
- [Zhang *et al.*, 2017a] Kaihao Zhang, Yongzhen Huang, Yong Du, and Liang Wang. Facial expression recognition based on deep evolutionary spatial-temporal networks. *IEEE Transactions on Image Processing*, 26(9):4193–4203, 2017.
- [Zhang *et al.*, 2017b] Zhifei Zhang, Yang Song, and Hairong Qi. Age progression/regression by conditional adversarial autoencoder. *arXiv preprint arXiv:1702.08423*, 2017.
- [Zhou and Shi, 2017] Yuqian Zhou and Bertram Emil Shi. Photorealistic facial expression synthesis by the conditional difference adversarial autoencoder. *arXiv preprint arXiv:1708.09126*, 2017.